

# Progress in heavy ion target capsule and hohlraum design

DEBRA A. CALLAHAN, MARK C. HERRMANN, AND MAX TABAK

Lawrence Livermore National Laboratory, Livermore, CA 94551 USA

## Abstract

Progress in heavy ion target design over the past few years has focused on relaxing the target requirements for the driver and for target fabrication. We have designed a plastic (CH) ablator capsule that is easier to fabricate and fill than the beryllium ablator we previously used. In addition, two-dimensional Rayleigh–Taylor instability calculations indicate that this capsule can tolerate ablator surface finishes up to 10 times rougher than the NIF specification. We have also explored the trade-off between surface roughness and yield as a method for finding the optimum capsule. We have also designed two new hohlraums: a “hybrid” target and a large-angle, distributed radiator target. The hybrid target allows a beam spot radius of almost 5 mm while giving gain of 55 from 6.7 MJ of beam energy in integrated Lasnex calculations. To achieve the required symmetry with the large beam spot, internal shields were used in the target to control the  $P_2$  and  $P_4$  asymmetry. The large-angle, distributed radiator target is a variation on the distributed radiator target that allows large beam entrance angles (up to  $24^\circ$ ). Integrated calculations have produced 340 MJ from 6.2 MJ of beam energy in a design that is not quite optimal. In addition, we have done a simple scaling to understand the peak ion beam power required to compress fuel for fast ignition using a short pulse laser.

**Keywords:** Heavy ion targets; Indirect drive; Inertial confinement fusion

## 1. INTRODUCTION

Designing a heavy ion fusion power plant will involve trading off requirements from targets, target fabrication, and chambers, as well as the accelerator driver. Our research program in target design is aimed at providing a range of options so that there is the flexibility to make these trade-offs between the different components of the power plant. To do this, we have been exploring a variety of capsule and hohlraum designs. In this article, we present a design for a new plastic capsule, which is easier to fabricate and fill than our previous beryllium capsule. Using two-dimensional, multimode Rayleigh–Taylor calculations on four variations of this capsule, we examine the trade-off between surface roughness and yield. We also present two hohlraum designs: a “hybrid” target as well as a large-angle version of the distributed radiator target. The hybrid target allows beam spots that are larger than previous designs, while the large-angle, distributed radiator target accepts large beam entrance angles.

In addition to this work with conventional, hot spot ignition targets, we have taken a preliminary look at reducing the peak ion beam power requirement with fast ignition

(Tabak *et al.*, 1994). For this study, we assumed the ion beams would compress the fuel, which would then be ignited by a short pulse laser. For a power plant, we will have to examine the trade-off between lower peak power for the accelerator with the cost/complexity of adding a short pulse laser to the system.

## 2. PLASTIC CAPSULE DESIGN

A capsule with a plastic (CH) ablator is better than one with a beryllium ablator for a power plant because it is easier to fabricate than a beryllium capsule and it can be filled with DT faster than a beryllium capsule (D.T. Goodin & A. Nobile, pers. comm.). For a power plant which requires  $\approx 500,000$  targets per day, a reduced filling time can significantly reduce the tritium inventory in the plant, making the plant safer (Latkowski *et al.*, 2001). In addition, target fabrication techniques developed for the ICF program can already produce CH shells with adequate surface finish (Takagi, 2001), although at smaller radius.

For a given drive temperature and capsule radius, we want to optimize the capsule design to give the largest yield taking into account Rayleigh–Taylor instability growth, achievable surface finishes, and beam power (i.e., drive temperature). Making the shell thicker means higher yield and less instability growth, but means the shell is moving

Address correspondence and reprint requests to: Debra A. Callahan, Lawrence Livermore National Laboratory, P.O. Box 808, L-015, Livermore, CA 94551, USA. E-mail: dcallahan@llnl.gov

**Table 1.** Parameters for the four plastic ablator capsules

Capsule	Very fast	Fast	Moderate	Slow
Ablator radius (mm)	2.30	2.28	2.30	2.34
Outer fuel radius (mm)	2.05	2.03	2.05	2.09
Inner fuel radius (mm)	1.82	1.74	1.70	1.68
Fuel mass (mg)	2.7	3.2	3.9	4.6
$v_{\text{imp-mw}} (\times 10^7 \text{ cm/s})$	3.1	2.8	2.5	2.3
Yield (MJ)	286	333	412	496
IFAR	50	45	38	26
Fuel Energy/ $E_{\text{ign}}$	1.8	1.6	1.3	1.1

slower and allows less margin (i.e., closer to the minimum energy for one-dimensional ignition). Faster, thinner shells have lower yield and more instability growth, but have more margin. A detailed description of the trade-off among margin, instability, growth and yield can be found in Herrmann *et al.* (2001).

To examine a specific example, we looked at four capsules. Each capsule had an outer radius of approximately 2.3 mm to compare with our previous beryllium ablator capsule and was driven at a peak temperature of 265 eV. The amount of fuel was varied between the four capsules to change the yield, implosion velocity, and shell thickness. Table 1 shows a summary of the capsule parameters.

The yield versus ablator roughness for these four capsules from multimode, two-dimensional Lasnex (Zimmerman & Krueger, 1975) calculations is shown in Figure 1. The bar at the left of the figure shows the surface roughness of mandrels that have been fabricated for NIF. For ablator roughness up to about two times this value (which may be reasonable given that our capsules are twice as large as NIF capsules), the slow capsule gives the highest yield.

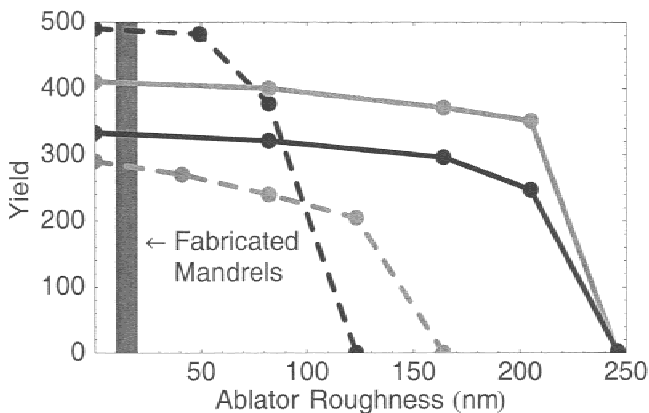


**Fig. 1.** Yield (in megajoules) versus ablator roughness (in nanometers) assuming  $1 \mu\text{m}$  ice roughness from multimode simulations of the four plastic ablator capsules. Very fast (dashed gray), fast (solid black), moderate (solid gray), and slow (dashed black).

These designs all used the same drive temperature. In the future, we will also explore the trade-off among drive temperature, surface roughness, and yield. In the end, we will give a maximum credible yield for a given surface finish and drive temperature. This will allow us the maximum flexibility for trading off capsule parameters.

### 3. HOHLRAUM DESIGN

Given an optimized capsule, the next step is to couple it to a hohlraum design to produce gain curves. The hohlraum design must integrate the requirements from the accelerator (e.g., beam power, beam distribution, spot size, entrance angles), the chamber (e.g., allowable materials, target injection accuracy), and target fabrication (fabrication tolerances, materials), in addition to target physics. To provide as many options as possible, we have worked on a variety of targets over the past several years including the distributed radiator target (Tabak *et al.*, 1998; Tabak & Callahan-Miller, 1998; Callahan-Miller & Tabak, 1999a) and the close-coupled target (Callahan-Miller & Tabak, 1999b, 2000). We present here two additional designs (or variations on a design): the hybrid target and the large-angle, distributed radiator target.

#### 3.1. Hybrid target design

The hybrid target is an option to allow a larger beam spot than previous targets. This target is a hybrid between the distributed radiator target (Tabak *et al.*, 1998; Tabak & Callahan-Miller, 1998; Callahan-Miller & Tabak, 1999a) and the end radiator target (Ho *et al.*, 1998) (thus the name “hybrid”) and allows a beam spot radius comparable to the hohlraum radius. This target is similar to the “foam” target of Honrubia *et al.* (1998). Figure 2 shows the geometry of the hybrid target. Note that the capsule used in the integrated calculations is the beryllium ablator capsule. In the future, we will integrate the results of the plastic ablator capsule optimization with the hohlraum design.

Two-dimensional, integrated Lasnex calculations of the hybrid target produce 370 MJ of yield from 6.7 MJ of beam energy (one-dimensional yield for this pulse shape is 410 MJ). These calculations assume the beams have a Gaussian distribution and are elliptical with semimajor and semiminor axes of 5.4 by 3.8 mm (this ellipse holds 9.5% of the charge). Although elliptical beams were used in these calculations, it may be possible to use round beams with this design, and future work will address this. As in our previous designs, the ion kinetic energy is changed between the foot of the pulse and the main pulse. In the calculation, the foot beams were assumed to be 3 GeV  $\text{Pb}^+$  ions in a  $6^\circ$  cone. The main pulse was assumed to be 4.5 GeV  $\text{Pb}^+$  ions in a  $12^\circ$  cone.

The notable features of this target are the internal shields used to control symmetry. Most of the beam energy is deposited behind a shine shield (region J in Fig. 2) and radi-

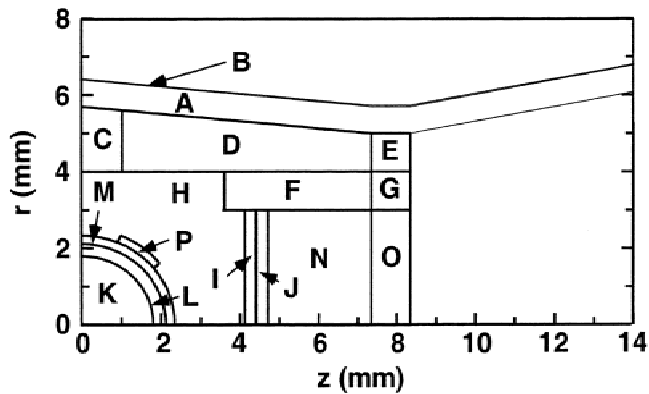


**Fig. 2.** A diagram of one-quarter of the capsule and hohlraum for the hybrid target. The complete target is a rotation about the  $z$ -axis and a reflection about the  $r$ -axis. The materials and densities used were as follows: (A) AuGd at 0.1 g/cc, (B) 15  $\mu\text{m}$  microns layer of AuGd at 13.5 g/cc, (C) Au at 32 mg/cc, (D)  $(\text{CD}_2)_{0.97}\text{Au}_{0.03}$  at 10 mg/cc, (E) AuGd at 0.1 g/cc, (F)  $(\text{CD}_2)_{0.97}\text{Au}_{0.03}$  at 40 mg/cc, (G) AuGd at 0.1 g/cc (upper half) and 0.2 g/cc (lower half), (H)  $\text{CD}_2$  at 1 mg/cc, (I) Al at 55 mg/cc (lower half) and 121 mg/cc (upper half), (J) Sn at 0.2 g/cc (lower half) and 0.3 g/cc (upper half), (K) DT at 0.3 mg/cc, (L) DT at 0.25 g/cc, (M)  $\text{Be}_{0.995}\text{Br}_{0.005}$  at 1.845 g/cc, (N) Al at 0.145 g/cc, (O) AuGd at 0.1 g/cc, (P) Fe at 10 mg/cc.

tion flows around the shine shield. The end result is that the capsule sees a bright source above the shine shield, which results in a significant  $P_4$  asymmetry. This is corrected using a shim (region P in Fig. 2)—a thin layer of iron placed on or near the capsule surface to block the excess energy.

Physics issues in the hybrid target include accurate calculation of hydrodynamic motion of the converter material and shine shield, accurate knowledge of the ion range, limits on the allowable beam angles, and the effect of the shim on the Rayleigh–Taylor instability.

In the hybrid target, pressure balance of the converter material had to be abandoned if we wanted to stop the ions behind the shine shield without increasing the hohlraum length. Increasing the hohlraum length would result in an additional energy penalty that we wanted to avoid. The end result is that both the converter and the shine shield expand radially during the pulse. If the shine shield expands too much, it blocks the path for radiation flow and results in poor coupling. If the converter expands too much, it intercepts more and more of the ions that are aimed above the shine shield and results in symmetry swings.

In the distributed radiator targets, the ion beam is aimed toward that hohlraum wall and away from the capsule, which made the target insensitive to small errors in ion range. In contrast, the hybrid target has the ion beam aimed directly at the capsule, and small errors in ion range can result in ions impacting the capsule. This must be avoided and so it is important to know the ion range (as a function of temperature and density) well for this target.

Another issue for the hybrid target is the allowable beam angles. Because the shine shield has to be large enough to protect the capsule, an increase in the beam angles will mean that a larger shine shield is needed. Using a larger shine shield will mean that more beam energy is deposited behind tile shield and make symmetry harder to achieve. A larger shine shield will increase the risk of having the gap between the shine shield and the wall close up as the shield expands during the pulse. In fact, the shine shield used in the integrated calculations was only big enough to protect the capsule from the  $6^\circ$  beams at time zero, when the target is cold and the ion range is long. The design used the fact that the ion range would be shorter and the shine shield would have expanded by the time the  $12^\circ$  cone of beams turned on in the main pulse.

The hybrid target uses a shim layer to correct the  $P_4$  asymmetry. In the integrated calculations, the shim was made up of a 200- $\mu\text{m}$ -thick layer of density 0.01 g/cc iron foam placed on the surface of the capsule. Placing the shim layer on the capsule can cause a perturbation that seeds the Rayleigh–Taylor instability. Capsule only calculations are now in progress to minimize the effect of the shim on the Rayleigh–Taylor instability.

The payoff for the target physics issues in the hybrid target is the large ion beam spot. The hybrid target requires 14% more beam energy than the distributed radiator target (6.7 MJ vs. 5.9 MJ), but the larger beam spot may mean that lighter, lower kinetic energy ions can be used. Lower kinetic energy means a shorter accelerator and may possibly be less expensive.

### 3.2. Large-angle, distributed radiator design

The beam geometry used in previous target designs assumed a fairly small number of beams ( $\sim 48$  beams) and used a very simple model for the amount of neutron shielding needed inside the final focus magnets. Recent work on the accelerator and chamber is pushing to larger numbers of beam, and detailed neutronics calculations of the final focus magnets suggest that more shielding is needed than was previously assumed. Both of these changes make the final focusing magnet array larger. Unless the size of the chamber is also increased, this means the beams will enter the target from larger angles than we have previously assumed.

Because the distributed radiator targets have the beams aimed away from the capsule, it should be relatively straightforward to allow larger beam angles in those targets. To do this, the hohlraum wall needs to be expanded over the capsule waist to prevent the large angle beams from hitting the wall. To accommodate beams at  $24^\circ$  (rather than the  $12^\circ$  used previously), the wall area needs to be increased by about 20%. Given that the wall loss is about 2.9 MJ out of a total of 5.9 MJ, we can estimate an additional energy penalty of about 600 kJ for a total energy of about 6.5 MJ.

Figure 3 shows the resulting hohlraum. Integrated Lasnex calculations have produced 340 MJ of yield in this geometry

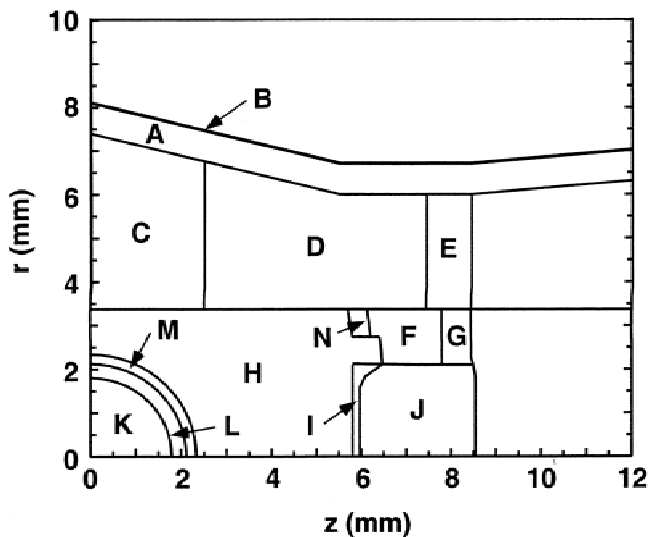


**Fig. 3.** A diagram of one-quarter of the capsule and holdraum for the large-angle, distributed radiator target. The complete target is a rotation about the  $z$ -axis and a reflection about the  $r$ -axis. The materials and densities used were as follows: (A) AuGd at 0.1 g/cc, (B) 15  $\mu\text{m}$  layer of AuGd at 13.5 g/cc, (C)  $(\text{CD}_2)_{0.97}\text{Au}_{0.03}$  at 32 mg/cc, (D)  $(\text{CD}_2)_{0.97}\text{Au}_{0.03}$  at 11 mg/cc, (E) AuGd at 0.11 g/cc, (F) Fe at 70 mg/cc, (G) AuGd at 0.26 g/cc, (H)  $\text{CD}_2$  at 1 mg/cc, (I) Al at 55 mg/cc, (J) AuGd sandwich with densities 0.1 g/cc, 1.0 g/cc, and 0.5 g/cc, (K) DT at 0.3 mg/cc, (L) DT at 0.25 g/cc, (M)  $\text{Be}_{0.995}\text{Br}_{0.005}$  at 1.845 g/cc, (N)  $(\text{CD}_2)_{0.97}\text{Au}_{0.03}$  at 32 mg/cc.

using four cones of ion beams per side. The inner two cones are used as foot beams using 3.3 GeV  $\text{Pb}^+$  ions. The inner most cone has 8 beams (per side) at an entrance angle of  $6^\circ$ . The next cone has 16 beams at an entrance angle of  $12^\circ$ . The two outer cones provide the main pulse, which uses 4 GeV  $\text{Pb}^+$  ions and has 24 beams at  $18^\circ$  and 32 beams at  $24^\circ$ . The integrated calculation used 6.2 MJ, but was driven at 245 eV rather than the 250-eV drive used in the original distributed radiator design. The symmetry is not yet optimal, as reflected in the fact that the one-dimensional yield for this pulse shape was 404 MJ.

Putting the foot beams at the inside of the array was necessary for symmetry considerations. With the large beam angles, the converter over the capsule waist (region C in Fig. 3) was quite large in radial extent. Using the large angle beams in the foot meant that the converter was only directly heated from the side closest to the hohlraum wall. Then, a large amount of converter material had to burn through before the capsule saw a source over the waist. This caused a very large time swing in the  $P_2$  asymmetry. This problem was corrected by using the shallow angle beams (two inner cones) for the foot.

One advantage to using the shallow angle beams for the foot was that we were able to use a 30% larger beam spot in the foot. The spots used in the integrated Lasnex calculations were elliptical with semiminor axis of 2.3 mm and semimajor axis of 4.2 mm in the foot and 1.8 mm by 4.2 mm in the main pulse. Recent work on chamber transport sug-

gests this is in the right direction; the foot beams are likely to be larger than the main pulse beams because the main pulse beams have extra neutralization in the chamber due to the photoionized plasma around the target. Since the foot beams heat the target to produce the photons, they do not benefit from this extra source of electrons and are not as well neutralized.

#### 4. HEAVY ION COMPRESSION FOR FAST IGNITION

In addition to work on conventional, hot spot targets, we have taken a preliminary look at using heavy ions to compress fuel for laser fast ignition.

The capsules used for this study were based on one-dimensional CH ablator designs. The first capsule was driven with a peak temperature of 150 eV for 17 ns. This capsule had an outer radius of 3.05 mm, an outer DT fuel radius of 2.93 mm, and an inner fuel radius of 2.78 mm. The central gas cavity had a little xenon gas added (atomic fraction  $1.3 \times 10^{-4}$ ) to radiatively cool the center and assist in forming a uniform density as a function of radius. In one dimension, the capsule absorbed 430 kJ of energy, reached an average density of 175 g/cc, and a  $\rho r$  of 3.3 g/cm<sup>2</sup>. Using a burn-up fraction of  $(\rho r)/(\rho r + 6)$ , we expect a yield of 460 MJ. We expect this capsule to require 50 kJ of ignitor energy deposited using Atzeni's formula (Atzeni, 1999) for the average density, which would mean a 150-kJ short pulse laser assuming 30% coupling efficiency.

The second capsule was driven with a peak temperature of 120 eV for 28 ns. It had an outer radius of 3.05 mm, an outer DT fuel radius of 2.95 mm, and an inner fuel radius of 2.8 mm. In one dimension, this capsule absorbed 260 kJ, reached an average density of 80 g/cc, and a  $\rho r$  of 2.25 g/cm<sup>2</sup>. We expect a yield from this  $\rho r$  of 350 MJ. Atzeni's formula with the average fuel density says that we would need 200 kJ of ignitor energy deposited or a 600-kJ short pulse laser assuming 30% coupling efficiency.

To estimate the ion beam energy and power required to compress these capsules, we used a one-sided hohlraum with converters at the zeros of the third Legendre polynomial (see Fig. 4). The capsule had a cone focus to minimize the plasma in the path of the shot pulse laser. Hatchett finds the best results for compressing cone-focus capsules when the drive has about a 10%  $P_1$  asymmetry; for the purposes of this simple scaling, the hohlraum is designed to be nearly symmetric.

The hohlraum radius is set by the capsule size (3 mm) plus the beam diameter. For this study, we assumed a beam radius of 2 mm. The total beam energy required was then estimated using  $E = E_{\text{wall}} + E_{\text{conv}} + E_{\text{cap}} + E_{\text{esc}}$  where the components are the wall loss energy, the converter energy, the capsule absorbed energy, and radiation escaped. The wall loss energy was  $E_{\text{wall}} \sim A_{\text{wall}} T_r^{3.3} \tau^{0.6}$  where  $A_{\text{wall}}$  is the wall area,  $T_r$  is the hohlraum temperature, and  $\tau$  is the pulse duration. The converter energy was  $E_{\text{conv}} \sim \pi r_h^2 RT$  where  $r_h$

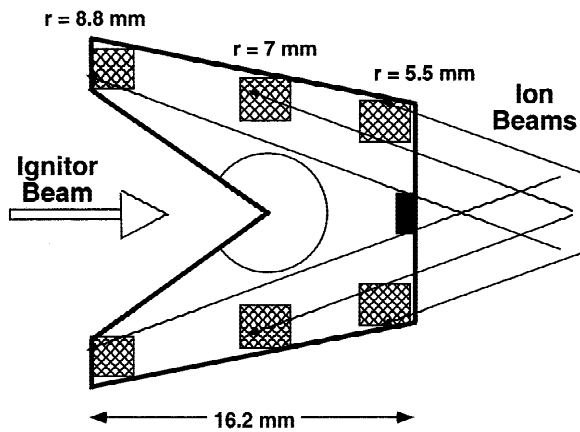


**Fig. 4.** A sketch of the hohlraum used for compressing a fast ignition capsule with heavy ions. The ion beams enter from the right and deposit their energy in converters located at the zeros of the third Legendre polynomial. An ignitor beam enters from the left.

was the hohlraum radius,  $R$  was the ion range, and  $T$  was the converter temperature. The capsule absorbed energy came from the one-dimensional calculations. The escaped energy was scaled using  $E_{\text{esc}} \sim A_{\text{enter}} T_r^4 \tau$  where  $A_{\text{enter}}$  was the entrance window area. As the hohlraum temperature changes, this formula is not quite correct. Ho *et al.* (1994) derived the energy lost through the entrance window including diffusion through the end shield plus the beam energy directly deposited there. For this case, the escaped energy is small ( $\approx 5\%$ ), so we will use this simpler approximation. The proportionality constants for these scalings was set based on our integrated calculations of the conventional distributed radiator target.

The result of this scaling is a drop in the ion beam power requirement. For the 150 eV capsule, compression would require 2.7 MJ and 160 TW of ion beam power. This would result in a gain of 160 with a 2.7-MJ ion beam compressor and a 150-kJ short pulse laser. For the 120-eV capsule, the compression would require 1.9 MJ and 68 TW of ion beam power. This would result in a gain of 140 with a 1.9-MJ ion beam compressor and a 600-kJ short pulse laser.

The results of this scaling are somewhat surprising. It is generally assumed that fast ignition produces very high gain at low driver energy. Yet, these results are not much better than the close-coupled target (gain 130 from 3.3 MJ of ion beam energy and 330 TW of power). Why is this? The lower hohlraum temperature reduces the wall loss drastically ( $T_r^{3.3}$ ) but the pulse duration is longer and the wall area is larger than for the close-coupled target. In addition, at low temperature, a considerable fraction of the energy ends up in the heat capacity of the converters (0.8 MJ out of 2.7 MJ for the 150-eV case).

This preliminary look at using an ion beam to compress fuel for fast ignition does show an advantage in the peak power required of the accelerator. We will have to assess whether this reduction in the peak power is enough to offset

the added complexity/cost of adding a short pulse laser to the power plant.

## 5. CONCLUSIONS

To design a heavy ion fusion power plant, we must be able to examine the trade-offs between the different components of the power plant. Our target design program is aimed at providing a range of options so that these trade-offs can be made. To this end, we have designed plastic ablator capsules which are easier to fabricate and fill than beryllium capsules. We have shown the trade-off between capsule surface finish requirements and yield for a set of four capsules. In the future, we will also examine the trade-off with drive temperature, which determines the required beam power.

Given an optimized capsule, a hohlraum needs to be designed which takes into account beam requirements (e.g., spot size and beam entrance angle), chamber requirements (e.g., hohlraum material choice), target fabrication (e.g., fabrication tolerances), and target physics (e.g., case-to-capsule ratio, symmetry techniques) to produce a gain curve. To expand the hohlraum design choices, we have presented two new designs: a hybrid target and a large-angle, distributed radiator target. The hybrid target allows large beam spots, but limited beam cone angles. The hybrid target also introduced new target physics issues including radiation flow around a shine shield, and a shim to correct asymmetry. The large-angle, distributed radiator target allows beam angles up to  $24^\circ$ , but with smaller beam spots.

In addition, we have taken a preliminary look at using ion beams to compress fuel for fast ignition by a short pulse laser. The required peak power from the accelerator was reduced by a factor of 2–5 from the close-coupled target for the examples we examined. The advantage of lower peak power will have to be traded off against the added cost/complexity of adding a short pulse laser for the ignitor.

## ACKNOWLEDGMENTS

This work was performed under the auspices of the U.S. Department of Energy by the University of California Lawrence Livermore National Laboratory under contact No. W-7405-ENG-48.

## REFERENCES

- ATZENI, S. (1999). Inertial fusion fast ignitor: Igniting pulse parameter window vs the penetration depth of the heating particles and the density of the precompressed fuel. *Phys. Plasmas* **6**, 3316–3326.
- CALLAHAN-MILLER, D.A. & TABAK, M. (1999a). A distributed radiator, heavy-ion target driven by Gaussian beams in a multi-beam illumination geometry. *Nucl. Fusion* **39**, 883–891.
- CALLAHAN-MILLER, D.A. & TABAK, M. (1999b). Increasing the coupling efficiency in a heavy-ion inertial confinement fusion target. *Nucl. Fusion* **39**, 1547–1556.

- CALLAHAN-MILLER, D.A. & TABAK, M. (2000). Progress in target physics and design for heavy ion fusion. *Phys. Plasmas* **7**, 2083–2091.
- HERRMANN, M.C., TABAK, M. & LINDL, J.D. (2001). Ignition scaling laws and their application to capsule design. *Phys. Plasmas* **8**, 2296–2304.
- HO, D.D.-M., LINDL, J.D. & TABAK, M. (1994). Radiation converter physics and a method for obtaining the upper limit for gain in heavy ion fusion. *Nucl. Fusion* **34**, 1081–1096.
- HO, D.D.-M., HARTE, J.A. & TABAK, M. (1998). Two dimensional simulations of a radiation driven target with two sided illumination for heavy ion fusion. *Nucl. Fusion* **38**, 701–710.
- HONRUBIA, J.J., RAMIS, R., RAMIREZ, J., MEYER-TER-VEHN, J., IBANEZ, L.F., PIRIZ, A.R., SANZ, J., SANCHEZ, M.M. & DE LA TORRE, M. (1998). Two-dimensional simulation of heavy ion hohlraum targets. *Nucl. Inst. Methods A* **415**, 104–109.
- LATKOWSKI, J.F., REYES, S., BESENBRUCH, G.E. & GOODIN, D.T. (2001). Preliminary safety assessment for an IFE target fabrication facility. *Fusion Technol.* **39**, 960–964.
- TABAK, M., HAMMER, J., GLINSKY, M.E., KRUER, W.L., WILKS, S.C., WOODWORTH, J., CAMPBELL, E.M., PERRY, M.D. & MASON, R.J. (1994). Ignition and high gain with ultrapowerful lasers. *Phys. Plasmas* **1**, 1626–1634.
- TABAK, M., CALLAHAN-MILLER, D., HO, D.D.-M. & ZIMMERMAN, G.B. (1998). Design of a distributed radiator target for inertial fusion driven from two sides with heavy ion beams. *Nucl. Fusion* **38**, 509–513.
- TABAK, M. & CALLAHAN-MILLER, D.A. (1998). Design of a distributed radiator target for inertial fusion driven from two sides with heavy ion beams. *Phys. Plasmas* **5**, 1896.
- TAKAGI, M., COOK, R., MCQUILLAN, D.B., ELSNER, F., STEPHENS, R., NIKROO, A., GIBSON, J. & PAGUIO, S. (2002). Development of high quality poly (alpha-methylstyrene) mandrels for NIF. *Fusion Technol.* **41**, 278–285.
- ZIMMERMAN, G.B. & KRUER, W.L. (1975). Numerical simulation of laser-initiated fusion. *Comments Plasma Phys. Controlled Fusion*, **2**, 51–61.